Progress of Theoretical Physics, Vol. 69, No. 4, April 1983

Gravitational Instabilities in a Dust-Gas Layer and Formation of Planetesimals in the Solar Nebula

Minoru SEKIYA

Department of Physics, Kyoto University, Kyoto 606

(Received November 22, 1982)

Dust particles which are initially distributed homogeneously in the solar nebula aggregate and settle towards the equatorial plane. As a result, the solar nebula separate into three layers: an equatorial thin dust-gas layer and two residual gas layers. We study gravitational instabilities in the dust-gas layer on the assumption of axial symmetry, taking account of motions perpendicular to as well as parallel to the equatorial plane and also making use of proper boundary conditions between the dust-gas layer and the gas layers.

As far as radii of dust particles are sufficiently small ($\lesssim 1$ cm at 1 au), a dust fluid and a gas fluid are firmly coupled owing to the drag force; consequently, they behave like one fluid. It is also found that the dust-gas layer behaves like an incompressible fluid owing to high pressure of the gas layers exerted on the dust-gas layer. Taking these conditions into account, a mode of gravitational instability accompanied with a motion perpendicular to the equatorial plane is newly found. If unstable wavelengths of the largest growing rate for non-axisymmetric and axisymmetric perturbations are the same, typical masses of planetesimals are 4×10^{17} g at the Earth orbit, 3×10^{20} g at the Jupiter orbit and 4×10^{21} g at the Neptune orbit.

§ 1. Introduction

Among various theories of formation of the solar system, theories based on a less massive nebula model with a mass of $0.01\sim0.04\ M_\odot$ have made remarkable achievements during the latest decade; formation mechanisms of the terrestrial and giant planets have been clarified;[1),2)] origin of the asteroids and satellites is also going to be explained.[3)] In contrast to stable, less massive nebula models, Cameron[4)] have proposed a massive solar nebula model with a mass of the order of $1\ M_\odot$; this massive nebula is unstable and breaks into gaseous giant protoplanets. The massive nebula model may result in formation of giant planets naturally; Cameron's theory seems to have, however, serious difficulties in explaining the formation processes of the asteroids and the satellites and also the dissipation mechanisms of the massive nebula and primitive atmospheres of the terrestrial planets and also of Uranus and Neptune. Among several less massive nebula models, we adopt in this paper the latest model by Hayashi.[5)] According to this model, surface density distribution is given by

$$\sigma_s = 1.7\times10^3\{r(\mathrm{au})\}^{-1.5}\ \mathrm{g\ cm^{-2}}. \tag{1·1}$$

Here, we briefly describe our scenario of the early evolutionary stage of the solar system. Initially, μ-sized dust particles floated homogeneously in the

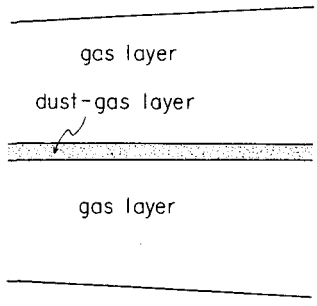

Fig. 1. The structure of the dust-gas layer and the gas layers in the solar nebula.

nebula. At that time, the ratio, ε, of the dust density, ρ_d, to the gas density, ρ_g, was as small as $1/57$ ($r>2.7$ au) and $1/240$ ($r<2.7$ au) according as water had been condensed or not, respectively. These dust particles aggregated and settled towards the equatorial plane. As a result, the solar nebula separated into three layers: an equatorial thin dust-gas layer and the two residual gas layers (Fig. 1).*) With sedimentation of dust particles, half thickness, h, of the dust-gas layer decreased. Simultaneously, dust density increased in inverse proportion to h. As a result, a greater part of dust particles were concentrated in the thin dust-gas layer. One should note that gas density was continuous without any gaps at the boundaries between the dust-gas layer and the gas layers.

Gravitational instability in the dust-gas layer is considered to have occurred when its density became sufficiently high. Fragmentation of the dust-gas layer due to self-gravity under the influence of the solar gravity and resultant formation of planetesimals were studied by Safronov,[1] Hayashi,[6] Goldreich and Ward,[7] and Coradini et al.[8] Safronov, and Goldreich and Ward supposed a fluid consisting of dust particles only, and neglected the effect of the gas contained in the dust-gas layer on the motion of the dust particles. This effect is, however, large in practice as seen later; therefore, the neglect of the gas effect is not reasonable. On the other hand, Hayashi[6] supposed a fluid composed of gas and dust which were coupled firmly owing to drag force. He derived a dispersion relation (referred to as the 2D mode) taking account of only the motion parallel to the equatorial plane. As seen in this paper, however, the motion perpendicular to the equatorial plane plays an essential role in the dynamics of the instability of the dust-gas layer. Recently, Coradini et al.[8] proposed two-fluid model of the dust-gas layer. They also restricted the fluid motion to be parallel to the equatorial plane. As a result, they found two typical modes; these are (1) a mode where dust fluid fragments through an unperturbed gas fluid (referred to as the type I mode after Coradini et al.[8]) and (2) the 2D mode mentioned above. The time scale of growth of the type I mode is, however, comparable to the sedimentation time of dust particles; therefore, it seems unsafe to neglect the dust sedimentation in deriving type I mode.

In this paper, dust and gas are assumed to be coupled firmly, and to be able

*) In practice, the boundary between the dust-gas layer and the gas layer was diffuse. We assume, however, the boundaries were sharp in order to simplify a mathematical treatment.

to be regarded as one fluid in order to avoid the complexity attributed to the relative motion of dust and gas. This assumption is good as far as the dust radius is smaller than the upper limit given in § 4. Further, we remove the restriction imposed by Hayashi, and Coradini et al. that the motion of the fluid is pallalel to the equatorial plane. In other words, a motion perpendicular to the equatorial plane is also taken into account. In addition, we consider the effect of pressure of the gas layers exerted on the dust-gas layer; i.e., proper boundary conditions between the dust-gas layer and the gas layers are used. As a result, we derive a new mode (referred to as the 3D mode) of gravitational instability in the dust-gas layer, after the analytical method by Goldreich and Lynden-Bell[9] (in the following, referred to as GL). This mode accompanies the motion perpendicular to the equatorial plane and bears resemblance to GL's incompressible mode. As seen in § 4, the 3D mode grows faster than the 2D mode.

§ 2. Basic equations

(a) *Equations for the dust-gas layer*

The dust-gas layer is composed of two fluids: a dust fluid and a gas fluid. They exert drag force and gravitational force with each other. We consider a case where a velocity difference of magnitude $\boldsymbol{u}$ between the dust fluid and the gas fluid is much less than the sound velocity of the gas and where the Reynolds number is much less than 10. In this case, the drag force exerted on the dust fluid per unit mass by the gas, $\boldsymbol{f}_D$, is given by[10]

$$\boldsymbol{f}_D = -\rho_g A \boldsymbol{u} . \tag{2·1}$$

The coefficient A is independent of $\boldsymbol{u}$ but depends on the Knudsen number: the ratio of the mean free path of gaseous molecules, l, to the radius of a dust particle, r_p. When $r_p < l$, the coefficient A is proportional to r_p^{-1}; the drag formula is

Table I. Gas density, ρ_g, mean free path of the gas molecules, l, and coefficient of the gas drag, A, at the Earth, Jupiter and Neptune orbits. For convenience of later use, values of A are given by the forms multiplied by $r_p\Omega^{-1}\rho_g$ and $r_p^2\Omega^{-1}\rho_g$ in the cases where $r_p \lesssim l$ and $r_p \gtrsim l$, respectively, where Ω is the Keplerian circular angular velocity. Hayashi's model gives $\rho_g \propto r^{-2.75}$ and $l \propto r^{2.75}$. We assume the mean molecular weight of the gas to be 2.34 and the mean collision cross section of molecules to be 2×10^{-15} cm^2. We also assume the solid density of dust particles to be 3.0 ($r<2.7$ au) and 1.0 ($r>2.7$ au).

Region (au)	ρ_g (gcm^{-3})	l (cm)	$\rho_g A r_p \Omega^{-1}$ ($r_p \lesssim l$) (cm)	$\rho_g A r_p^2 \Omega^{-1}$ ($r_p \gtrsim l$) (cm^2)
Earth (1.0)	1.4×10^{-9}	1.4	3.6×10^{2}	7.8×10^{2}
Jupiter (5.2)	1.5×10^{-11}	1.3×10^{2}	9.1×10	1.8×10^{4}
Neptune (30.2)	1.2×10^{-13}	1.7×10^{4}	6.5	1.7×10^{5}

reduced to Epstein's law. Conversely, if $r_p > l$, A is proportional to r_p^{-2}; Eq. (2·1) is reduced to Stokes' law. Table I gives values of A at the orbits of the Earth, Jupiter and Neptune.

Consider the Sun to be at the origin of the cylindrical coordinate system (r, ϕ, z) with z measured from the equatorial plane of the solar nebula. The two fluids revolving around the Sun are described by the following equations on the assumptions of axi-symmetry ($\partial/\partial\phi = 0$):

$$\frac{\partial u_d}{\partial t} + u_d\frac{\partial u_d}{\partial r} + w_d\frac{\partial u_d}{\partial z} - \frac{v_d^2}{r} = -\Omega^2 r - \frac{\partial \psi}{\partial r} - \rho_g A(u_d - u_g), \quad (2\cdot2)$$

$$\frac{\partial v_d}{\partial t} + u_d\frac{\partial v_d}{\partial r} + w_d\frac{\partial v_d}{\partial z} + \frac{u_d v_d}{r} = -\rho_g A(v_d - v_g), \quad (2\cdot3)$$

$$\frac{\partial w_d}{\partial t} + u_d\frac{\partial w_d}{\partial r} + w_d\frac{\partial w_d}{\partial z} = -\Omega^2 z - \frac{\partial \psi}{\partial z} - \rho_g A(w_d - w_g), \quad (2\cdot4)$$

$$\frac{\partial \rho_d}{\partial t} + \frac{\partial}{\partial r}(\rho_d u_d) + \frac{\partial}{\partial z}(\rho_d w_d) + \frac{\rho_d u_d}{r} = 0, \quad (2\cdot5)$$

$$\frac{\partial u_g}{\partial t} + u_g\frac{\partial u_g}{\partial r} + w_g\frac{\partial u_g}{\partial z} - \frac{v_g^2}{r} = -\Omega^2 r - \frac{\partial \psi}{\partial r} - \frac{1}{\rho_g}\frac{\partial P_g}{\partial r} - \rho_d A(u_g - u_d), \quad (2\cdot6)$$

$$\frac{\partial v_g}{\partial t} + u_g\frac{\partial v_g}{\partial r} + w_g\frac{\partial v_g}{\partial z} + \frac{u_g v_g}{r} = -\rho_d A(v_g - v_d), \quad (2\cdot7)$$

$$\frac{\partial w_g}{\partial t} + u_g\frac{\partial w_g}{\partial r} + w_g\frac{\partial w_g}{\partial z} = -\Omega^2 z - \frac{\partial \psi}{\partial z} - \frac{1}{\rho_g}\frac{\partial P_g}{\partial z} - \rho_d A(w_g - w_d), \quad (2\cdot8)$$

$$\frac{\partial \rho_g}{\partial t} + \frac{\partial}{\partial r}(\rho_g u_g) + \frac{\partial}{\partial z}(\rho_g w_g) + \frac{\rho_g u_g}{r} = 0, \quad (2\cdot9)$$

$$P_g = \varkappa_g \rho_g^{\gamma}, \quad (2\cdot10)$$

$$\left(\frac{1}{r}\frac{\partial}{\partial r}r\frac{\partial}{\partial r} + \frac{\partial^2}{\partial z^2}\right)\psi = 4\pi G(\rho_d + \rho_g). \quad (2\cdot11)$$

Here, u, v and w are the r-, ϕ- and z-components of the velocity, respectively; the subscripts d and g refer to quantities of the dust and the gas, respectively; t denotes the time; ψ the gravitational potential of the dust-gas layer; P_g the gas pressure. In the above, the polytropic equation of state is assumed for the gas fluid; on the other hand, the dust pressure is neglected, since this is sufficiently small in our case. The solar gravity is simply written as $\Omega^2 r$ and $\Omega^2 z$ (Ω being the Keplerian angular velocity of a circular orbit, $(G\,M_\odot/r^3)^{1/2}$), because of the smallness of $z^2/r^2 (\lesssim 10^{-10})$.

In the following, we restrict ourselves to a case where relative velocity of the dust fluid to the gas fluid is very small owing to a strong drag force. In other

words, we consider a phenomenon with a time scale much shorter than the separation time of the dust fluid and the gas fluid (examination on this assumption will be made in § 4). Mathematically, this assumption corresponds to the limiting case where $u_d \to u_g$, $v_d \to v_g$, $w_d \to w_g$ and $A \to \infty$. In this case, Eqs. (2·2)~(2·11) are reduced to the following one-fluid equations:

$$\frac{\partial U}{\partial t}+U\frac{\partial U}{\partial r}+W\frac{\partial U}{\partial z}-\frac{V^2}{r}=-\Omega^2 r-\frac{\partial \psi}{\partial r}-\frac{1}{\rho}\frac{\partial P}{\partial r}, \tag{2·12}$$

$$\frac{\partial V}{\partial t}+U\frac{\partial V}{\partial r}+W\frac{\partial V}{\partial z}+\frac{UV}{r}=0, \tag{2·13}$$

$$\frac{\partial W}{\partial t}+U\frac{\partial W}{\partial r}+W\frac{\partial W}{\partial z}=-\Omega^2 z-\frac{\partial \psi}{\partial z}-\frac{1}{\rho}\frac{\partial P}{\partial z}, \tag{2·14}$$

$$\frac{\partial \rho}{\partial t}+\frac{\partial}{\partial r}(\rho U)+\frac{\partial}{\partial z}(\rho W)+\frac{\rho U}{r}=0, \tag{2·15}$$

$$P=\varkappa\rho^{\gamma}, \tag{2·16}$$

$$\left(\frac{1}{r}\frac{\partial}{\partial r}r\frac{\partial}{\partial r}+\frac{\partial^2}{\partial z^2}\right)\psi=4\pi G\rho, \tag{2·17}$$

where

$$U=u_d=u_g, \tag{2·18}$$

$$V=v_d=v_g, \tag{2·19}$$

$$W=w_d=w_g, \tag{2·20}$$

$$\rho=\rho_d+\rho_g, \tag{2·21}$$

$$P=P_g, \tag{2·22}$$

$$\varkappa=\varkappa_g(1+\varepsilon)^{-\gamma} \tag{2·23}$$

and

$$\varepsilon=\rho_d/\rho_g. \tag{2·24}$$

We assume that ε is a constant throughout the dust-gas layer in order to simplify a mathematical treatment.

(b) *Unperturbed state*

Before deriving perturbation equations, we describe the unperturbed state adopted here, which is hereafter denoted by the subscript 0. As seen later, wavelength of the most unstable mode as well as a thickness of the dust-gas layer is sufficiently smaller than r. Therefore, we can replace r by $\hat{r}$, $\Omega(r)$ by $\Omega(\hat{r})$

and $\partial[r\Omega(r)]/\partial r$ by $-\Omega(\hat{r})/2$, where $\hat{r}$ is a characteristic heliocentric distance of the region under consideration. We also neglect the dependence of ρ_0 and P_0 on r and take values at $\hat{r}$; their distributions are assumed to be symmetric with respect to the equatorial plane.

In this case, unperturbed gravitational potential, ψ_0, is given by that of an infinite disk spreading uniformly over the radial direction, i.e.,

$$d\psi_0/dz = 2\pi G\sigma_0(z), \tag{2·25}$$

where

$$\sigma_0(z) = 2\int_0^z \rho_0 dz\,. \tag{2·26}$$

The components of a velocity are assumed to be equal to those of Keplerian circular motion, i.e.,

$$(U_0,\ V_0,\ W_0) = (0,\ \Omega r,\ 0). \tag{2·27}$$

Therefore, ρ_0 and P_0 are independent of time as seen from Eqs. (2·15) and (2·16). Lastly, the remaining equations (2·14) and (2·16) become

$$0 = -\Omega^2 z - \frac{d\psi_0}{dz} - \frac{1}{\rho_0}\frac{dP_0}{dz} \tag{2·28}$$

and

$$P_0 = \varkappa\rho_0{}^{\gamma}\,, \tag{2·29}$$

respectively. Equation (2·28) means that pressure gradient of the gas is in equilibrium with the sum of gravitational forces exerted on both dust and gas.

(c) *Perturbation equations*

Now, we will derive perturbation equations from Eqs. (2·12)~(2·17) taking the first order terms of small perturbations (subscript 1). By means of the usual manner, we have

$$\frac{\partial U_1}{\partial t} - 2\Omega V_1 = -\frac{\partial}{\partial r}\left(\psi_1 + \frac{P_1}{\rho_0}\right), \tag{2·30}$$

$$\frac{\partial V_1}{\partial t} + \frac{1}{2}\Omega U_1 = 0\,, \tag{2·31}$$

$$\frac{\partial W_1}{\partial t} = -\frac{\partial}{\partial z}\left(\psi_1 + \frac{P_1}{\rho_0}\right), \tag{2·32}$$

$$\frac{\partial \rho_1}{\partial t} + \rho_0\frac{\partial U_1}{\partial r} + \frac{\partial}{\partial z}(\rho_0 W_1) + \frac{\rho_0 U_1}{r} = 0\,, \tag{2·33}$$

$$P_1 = c_0^2 \rho_1 , \tag{2·34}$$

$$\left(\frac{1}{r} \frac{\partial}{\partial r} r \frac{\partial}{\partial r} + \frac{\partial^2}{\partial z^2} \right) \psi_1 = 4\pi G \rho_1 , \tag{2·35}$$

where c_0 is the sound velocity of the dust-gas fluid, i.e.,

$$c_0^2 = \varkappa \gamma \rho_0^{\gamma - 1} . \tag{2·36}$$

As seen from Eq. (2·23), the sound velocity of a dust-gas fluid, c_0, is $(1+\varepsilon)^{-1/2}$ times as large as the sound velocity of the gas, c_{g0}, which is given by

$$c_{g0}^2 = \varkappa_g \gamma \rho_{g0}^{\gamma - 1} . \tag{2·37}$$

Denoting

$$f = -\partial [\psi_1 + (P_1/\rho_0)]/\partial r , \tag{2·38}$$

$$g = -\partial \psi_1 / \partial r , \tag{2·39}$$

$$W_r = \partial W_1 / \partial r \tag{2·40}$$

and

$$\rho_r = \partial \rho_1 / \partial r , \tag{2·41}$$

and assuming a form like $U_1 = \tilde{U}(z) J_1(kr) e^{-i\omega t}$, we finally obtain the following equations from Eqs. (2·30)~(2·35):

$$-i\omega \tilde{U} - 2\Omega \tilde{V} = \tilde{f} , \tag{2·42}$$

$$-i\omega \tilde{V} + (1/2)\Omega \tilde{U} = 0 , \tag{2·43}$$

$$-i\omega \tilde{W}_r = d\tilde{f}/dz , \tag{2·44}$$

$$-i\omega \tilde{\rho}_r - k^2 \rho_0 \tilde{U} + d(\rho_0 \tilde{W}_r)/dz = 0 , \tag{2·45}$$

$$\tilde{g} - \tilde{f} = (c_0^2/\rho_0) \tilde{\rho}_r , \tag{2·46}$$

$$[-k^2 + (d^2/dz^2)] \tilde{g} = -4\pi G \tilde{\rho}_r . \tag{2·47}$$

§ 3. The 2D mode

Here, we briefly review the 2-dimensional (2D) mode of instability in order to compare with the 3D mode of instability which will be derived in § 4. In order to simplify a mathematical treatment, we assume that c_0^2 and ρ_0 depend very weakly on z. As seen in Appendix(a), this assumption is consistent with constancy of ε which has been assumed in § 2. We further assume that the fluid motion is restricted to be parallel to the equatorial plane, i.e., $W_1 = 0$. Putting $\tilde{W}_r = 0$, we get the following equations for 2D mode from Eqs. (2·42), (2·43) and

(2·45)~(2·47):

$$-i\omega\tilde{U}-2\Omega\tilde{V}=\tilde{f}\,, \tag{3·1}$$

$$-i\omega\tilde{V}+(1/2)\Omega\tilde{U}=0\,, \tag{3·2}$$

$$-i\omega\tilde{\rho}_{\mathrm{r}}-k^2\rho_0\tilde{U}=0\,, \tag{3·3}$$

$$\tilde{g}-\tilde{f}=(c_0{}^2/\rho_0)\tilde{\rho}_{\mathrm{r}}\,, \tag{3·4}$$

$$[-k^2+(d^2/dz^2)]\tilde{g}=-4\pi G\tilde{\rho}_{\mathrm{r}}\,. \tag{3·5}$$

We assume here that $\tilde{g}(z)$ and $\tilde{\rho}_{\mathrm{r}}(z)$ are proportional to $\cos(Lz/h)$ or $\sin(Lz/h)$ in the range $-h<z<h$; while, in the range $|z|>h$, $\tilde{g}$ is proportional to $\exp(-k|z|)$. The boundary condition imposed on the gravitational potential is deduced from continuity of $\tilde{g}'(z)/\tilde{g}(z)$ at $|z|=h$, i.e.,

$$L\cdot\tan L=K\,, \tag{3·6}$$

for cosine mode and

$$L\cdot\cot L=-K\,, \tag{3·7}$$

for sine mode, where $K=kh$. As is easily seen, we have infinite number of eigenvalues of L. From Eq. (3·5), the relation between $\tilde{g}$ and $\tilde{\rho}_{\mathrm{r}}$ is given by

$$\tilde{g}=(4\pi Gh/k)F(K)\tilde{\rho}_{\mathrm{r}}\,, \tag{3·8}$$

where

$$F(K)=K/(K^2+L^2). \tag{3·9}$$

We are of course interested in the most rapidly growing mode of instabilities. As seen from Eqs. (3·8) and (3·9), $\tilde{g}$ increases with the decrease in the value of L; hence, the maximum growth rate is expected to be realized for the minimum eigenvalue, i.e., the eigenvalue of the cosine mode in the range $0<L<\pi/2$ (as seen from Eq. (3·7), no eigenvalues are found in the range $0<L<\pi/2$ for the sine mode). In this case, the asymptotic forms of Eq. (3·9) are very simple. If $K\ll 1$, we have $L^2\approx K$ from Eq. (3·6); therefore $F(K)\approx 1$. On the other hand, if $K\gg 1$, Eq. (3·6) leads to $L\approx\pi/2$; therefore $F(K)\approx 1/K$.

Now, the dispersion relation for the 2D mode[6] is derived from Eqs. (3·1) ~(3·4) and (3·8), i.e.,

$$\omega^2=c_0{}^2k^2-2\pi G\sigma_0F(K)k+\Omega^2\,, \tag{3·10}$$

where $\sigma_0=2\rho_0h$. As seen just below, this mode does not grow till the dust-gas layer becomes extremely thin, i.e., ε becomes sufficiently high. In this case, we have $F(K)=1$, since $K\ll 1$. The conditions for the critical stability (denoted by

Table II.(a) The values of ε, h and λ at the marginal stability of the 2D mode.

Region	ε_c	h_c (cm)	λ_c (cm)
Earth	2.5×10^{8}	1.0×10	2.4×10^{8}
Jupiter	6.2×10^{6}	1.4×10^{4}	1.2×10^{10}
Neptune	2.6×10^{6}	2.9×10^{5}	1.7×10^{11}

the subscript c), i.e., $\omega=\partial\omega/\partial k=0$, are given by

$$\varepsilon_c=(c_{g0}\Omega/\pi G\sigma_0)^2-1 \tag{3·11}$$

and

$$k_c=\Omega^2/\pi G\sigma_0\,. \tag{3·12}$$

Table II(a) gives values of ε_c, h_c (being the critical thickness of the dust-gas layer) and λ_c ($=2\pi/k_c$) at the orbits of the Earth, Jupiter and Neptune. In all the regions, the critical value of ε_c (or h_c) is surprisingly large (or small); hence, the 3D mode of instability, mentioned in the next section, certainly overcomes the 2D mode.

§ 4. The 3D mode

Here, a mode of gravitational instability in the dust-gas layer including a motion perpendicular to as well as parallel to the equatorial plane (i.e., the 3D mode) is derived. We hereafter assume that the dust-gas fluid behaves like an incompressible fluid. In other words, we consider the limiting case where $c_0\to\infty$ and $\tilde{\rho}_r\to0$. This approximation is very good for the dust-gas fluid under consideration as seen in Appendix(a). Further, we neglect the z-dependence of ρ_0; this assumption is consistent with the one that ε is constant throughout the dust-gas layer as seen in Appendix(a). In this case, the surface density, $\sigma_0(h)$, is simply given by

$$\sigma_0(h)=2\rho_0 h\,. \tag{4·1}$$

On these assumptions, we obtain the following equations for the dust-gas fluid from Eqs. (2·42)~(2·45) and (2·47), i.e.,

$$-i\omega\tilde{U}-2\Omega\tilde{V}=\tilde{f}\,, \tag{4·2}$$

$$-i\omega\tilde{V}+(1/2)\Omega\tilde{U}=0\,, \tag{4·3}$$

$$-i\omega\tilde{W}_r=d\tilde{f}/dz\,, \tag{4·4}$$

$$-k^2\tilde{U}+d\tilde{W}_r/dz=0\,, \tag{4·5}$$

$$[-k^2+(d^2/dz^2)]\tilde{g}=0\,. \tag{4·6}$$

Note that the equation of state, (2·46), is replaced by the equation $\tilde{\rho}_1=0$.

In order to obtain a dispersion relation, boundary conditions between the dust-gas and the gas layers must be imposed. In the following, we will consider only a mode symmetric with respect to the equatorial plane, since asymmetric modes are always stable as shown by GL. In this case, it is sufficient for us to give boundary conditions at the boundary in the region $z>0$, although there are two boundaries with their unperturbed coordinates, $z=h$ and $z=-h$. Denoting the displacement of the boundary perpendicular to the equatorial plane by δ_1, we obtain the following equation within the same order of accuracy as the perturbed quantities, i.e.,

$$\partial^2\delta_1/\partial t^2=\partial W_1/\partial t|_h\,. \tag{4·7}$$

Putting

$$\delta_1=\partial\delta_1/\partial r=\tilde{\delta}_1 J_1(kr)e^{-i\omega t}\,, \tag{4·8}$$

and using Eq. (4·4), we have the equation describing the motion of the boundary, i.e.,

$$-i\omega^2\tilde{\delta}_1=(d\tilde{f}/dz)_h\,. \tag{4·9}$$

The boundary condition that the gas pressure should be continuous between the gas layer and the dust-gas layer is given by

$$P_g(h+\delta_1)=P_{ge}\,, \tag{4·10}$$

where P_{ge} is the pressure of the gas layer at the boundary. We can neglect the change of the value of P_{ge} due to displacement of the boundary as shown in Appendix(b). Then, Eqs. (4·10) and (2·22) lead to

$$\begin{aligned}P_g(h)&=P_{g0}(h)+P_{g1}(h)=P_{ge}+P_{g1}(h)\\&=P_g(h+\delta_1)+P_1(h).\end{aligned} \tag{4·11}$$

The equation of motion of a fluid element in the range $h<z<h+\delta_1$ (if $\delta_1<0$, suppose a fluid element with negative density in the range $h+\delta_1<z<h$) is given by

$$\rho_0\frac{dW}{dt}=\rho_0\left(-\frac{\partial\psi}{\partial z}-\Omega^2 z\right)-\frac{\partial P_g}{\partial z}\,. \tag{4·12}$$

Integrating this equation from h to $h+\delta_1$, neglecting higher order terms of perturbed quantities and using Eq. (4·11), we get

$$P_1(h)=\rho_0[(d\psi_0/dz)_h+\Omega^2 h]\delta_1\,. \tag{4·13}$$

Eliminating σ_0, P_1, ψ_1 and ψ_0 from Eqs. (2·25), (2·38), (2·39), (4·1) and (4·13), and

performing the Fourier-Bessel transformation, we finally obtain

$$\tilde{g}(h)-\tilde{f}(h)=\tilde{\delta}_r(4\pi G\rho_0+\Omega^2)h\,. \tag{4·14}$$

The boundary condition to be imposed on the gravitational potential has been already given by Eq. (53) in GL and is rewritten in our case as

$$(d\tilde{g}/dz)_h-4\pi G\rho_0\tilde{\delta}_r+k\tilde{g}(h)=0\,. \tag{4·15}$$

The perturbation equations and the boundary conditions described above are almost the same as those given by GL for a rigidly rotating disk of an incompressible fluid except for the following two points: (1) the term, 2Ω, in GL's Eq. (89) is replaced by $\Omega/2$ as Eq. (4·3) owing to the difference between the rigid and differential rotations; (2) the z component of the solar gravity, $\Omega^2 h$, is added in the pressure boundary condition as Eq. (4·14).

By means of calculations similar to those made by GL, a dispersion relation can be deduced from Eqs. (4·2)~(4·6), (4·9), (4·14) and (4·15),

$$\omega^2=\left\{\left[1-\frac{1+e^{-2K}}{2K}\right]4\pi G\rho_0+\Omega^2\right\}nK\cdot\mathrm{th}(nK), \tag{4·16}$$

where $n^2=[1-(\Omega^2/\omega^2)]^{-1}$ and $K=kh$. Note that in the case where $0<\omega^2<\Omega^2$, n is a pure imaginally number; the term $nK\cdot\mathrm{th}(nK)$ in Eq. (4·16) should be replaced by $-mK\cdot\tan(mK)$, where $m^2=[(\Omega^2/\omega^2)-1]^{-1}$.

At the marginal stability (denoted by the subscript c), we have $K_c=0.2775$ and $(4\pi G\rho_0/\Omega^2)_c=7.617$; i.e., $k_c=1.057\Omega^2/\pi G\sigma_0$ and $\rho_{0c}=0.17\rho_R$, where ρ_R ($=3.534\times M_\odot/r^3$) is Roche's density.[11] Thus, the critical wave number of the 3D mode is almost equal to that of the 2D mode (see Eq. (3·12)). On the other hand, the critical density of the 3D mode is much less than that of the 2D mode. In Table II(b), the values of ε_c, h_c and λ_c are given. Since $\lambda_c/r\ll 1$ as seen from Table II(b), the adopted assumption that Ω, $\partial(r\Omega)/\partial r$, ρ_0 and P_0 are all independent of r is justified with a good accuracy. Denoting the critical wavelength of non-axisymmetric mode as $\xi\lambda_c$, about which we have little knowledge, a mass of a fragment is given by $M_c=\xi\lambda_c^2\sigma_0$. Table II(b) also gives values of M_c in the case where $\xi=1$.

In Fig. 2, dispersion relations of the 3D mode are illustrated for the two cases where the minimum values of ω^2 are equal to 0 (i.e., the marginal stability, which is denoted by A) and to $-\Omega^2$ (denoted by B). A perturbed state with a small

Table II.(b) The values of ε, h and λ at the marginal stability of the 3D mode. Masses of the planetesimals are also given.

Region	ε_c	h_c (cm)	λ_c (cm)	mass (g)
Earth	2.6×10^2	9.9×10^6	2.2×10^8	3.5×10^{17}
Jupiter	1.7×10^2	4.9×10^8	1.1×10^{10}	3.2×10^{20}
Neptune	1.1×10^2	6.9×10^9	1.6×10^{11}	4.4×10^{21}

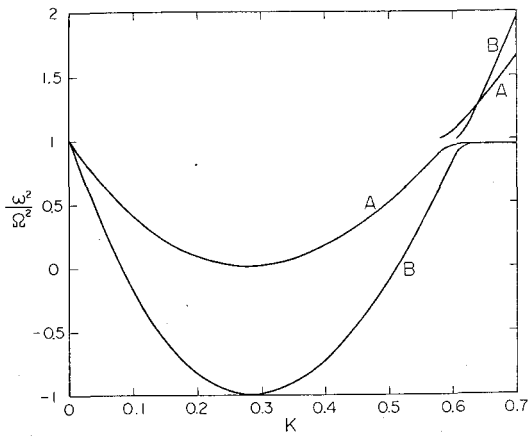

Fig. 2. Dispersion relations of the 3D modes are shown for the case where (A) $4\pi G\rho_0/\Omega^2=7.6169$ ($\omega^2_{\min}=0$) and (B) $4\pi G\rho_0/\Omega^2=14.875$ ($\omega^2_{\min}=-\Omega^2$).

wave number is stabilized owing to tidal force by the Sun; in the limit $k\to 0$, we have $|\omega|\to\Omega$. On the other hand, a perturbed state with large wave number is again stabilized by z-components of the solar gravity and of the self-gravity. The term $\{\cdots\}$ in Eq. (4·16) is an increasing function of K and is positive for K larger than a critical value K^*. The value of K^* depends on the value of $4\pi G\rho_0/\Omega^2$ ($K^*=0.5804$ (A), 0.6075 (B)). In Fig. 2, only a mode with $0<mK<\pi$ is illustrated for $0<\omega^2<\Omega^2$.

In Fig. 3, the values of $|\omega|/\Omega$ for 3D mode as well as those for 2D mode with a wave number where ω^2 (<0) has the minimum value, i.e., the maximum growing rate, are illustrated. Figure 3 also shows sedimentation rate ω_s of the dust particles, i.e.,

$$\omega_s/\Omega=[1+(4\pi G\rho/\Omega^2)]/(\rho_g A/\Omega), \qquad (4\cdot 17)$$

where values of $\rho_g A/\Omega$ is given in Table I. From this figure, we find that 3D mode grows faster than the sedimentation of the dust particles, as far as the dust

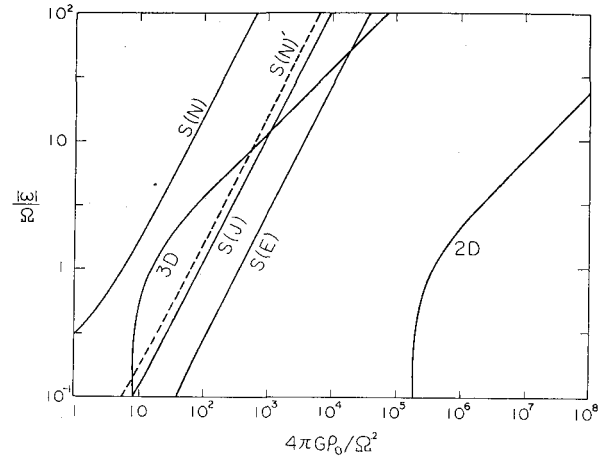

Fig. 3. The growth rate of the 2D and 3D modes. Sedimentation rates of dust particles with the radii of 1 cm (denoted by S) and 1 mm (denoted by S′) are also given, where the Earth, Jupiter and Neptune orbits are referred to as E, J and N, respectively.

radii are smaller than 1 cm at the Earth and the Jupiter orbits and than 1 mm at the Neptune orbit.*) While, the growth rate ω_I of the type I mode (see § 1) is given by[8]

$$\omega_I/\Omega=(4\pi G\rho/\Omega^2)/(\rho_g A/\Omega). \tag{4·18}$$

Since $\omega_I<\omega_s$, we can also neglect the radial migration of the dust fluid through the gas fluid as far as the dust radius is smaller than the value given above. Further, we can see from this figure that 3D mode grows with a sufficiently large rate at a density below the critical density for growth of the 2D mode. Therefore, we can conclude that 3D mode derived in this paper is the most probable mode of the fragmentation of the dust-gas layer in the solar nebula.

Lastly, we speculate the further fate of the dust-gas layer after the beginning of the growth of the 3D mode. The fragment composed of the dust and the gas probably approaches a stable configuration, where the solar and the self-gravities are balanced with the centrifugal force, conserving angular momentum, mass and also volume owing to its incompressibility in a short time scale of the order of 1 yr. Next stage lasts rather longer where dust particles settle towards the center of the fragment. As a result, solid planetesimals are formed. Therefore the formation time of planetesimals is of the order of the sedimentation time of the dust particles. It should be noted, however, that the mass of the fragment is determined by the 3D mode.

Acknowledgements

The author is grateful to Professor C. Hayashi for stimulating discussion and continuous encouragement, and to Professor K. Nakazawa for a critical reading of the manuscript. He also wishes to thank Professor H. Sato and Dr. T. Nakamura for helpful comments.

Appendix

(a) *Incompressibility*

We neglected $\tilde{\rho}_r$ in Eqs. (2·45) and (2·47) when we derived Eqs. (4·5) and (4·6). Here, this neglect is assured. Using Eq. (2·46), we have

$$|i\omega\tilde{\rho}_r/\rho_0 k^2\tilde{U}|=|\omega(\tilde{g}-\tilde{f})/c_0^2 k^2\tilde{U}| \tag{A·1}$$

*) Nakagawa et al.[12] estimated the dust radius to be 22 cm (Earth), 7.5 cm (Jupiter) and 0.86 cm (Neptune) at Roche's density assuming the sticking probability to be unity. The accurate values of the dust radius are, however, not be able to be estimated without a precise knowledge of the sticking probability.

and

$$|4\pi G\tilde{\rho}_r/k^2\tilde{g}|=|4\pi G\rho_0(\tilde{g}-\tilde{f})/c_0^2k^2\tilde{g}|. \qquad (A\cdot 2)$$

We will show that these are much smaller than unity. As for the 3D mode, we have from Eqs. (4·2) and (4·3) that $\tilde{U}\sim\tilde{f}/\Omega$ when $\omega\sim\Omega$; further we note that $\tilde{f}\sim\tilde{g}\sim(\tilde{g}-\tilde{f})$. Noticing that $4\pi G\rho_0\sim\Omega^2$ for the density of the order of Roche's density and that $kh=O(1)$ for the most unstable wavelength, we obtain

$$|i\omega\tilde{\rho}_r/\rho_0k^2\tilde{U}|\sim|4\pi G\tilde{\rho}_r/k^2\tilde{g}|\sim\Omega^2h^2/c_0^2\,. \qquad (A\cdot 3)$$

At the marginal stability of the 3D mode, the values of Ω^2h^2/c_0^2 are equal to 7×10^{-8} (for the Earth region), 2×10^{-6} (Jupiter) and 3×10^{-6} (Neptune). This means that the approximation of incompressibility is very good.

We also see from the above result that the density scale height c_0/Ω is much larger than half thickness of the dust-gas layer h. Therefore ρ_0 depends very weakly on z for the 3D mode as far as ε is independent of z. In other words, the neglect of the z-dependence of ρ_0 is consistent with the assumption that ε is constant. This consistency is also held for the 2D mode, since the ratio of the half thickness of the dust-gas layer to the density scale height, $G\sigma_0h/c_0^2$, scarcely depends on h.

(b) *Change of the pressure of the gas layer at the boundary*

We show here that the change of the value of P_{ge} can be neglected. The flow velocity of the gas, v_g, due to the motion of the boundary between the dust-gas layer and a gas layer is of the order of $\lambda\omega$, where λ is the wave length ($=2\pi/k$). In the case where $\omega\sim\Omega$, we have $v_g\sim\lambda\Omega$. Therefore values of the ratio of the flow velocity to the sound velocity v_g/c_{g0} are of the order of 4×10^{-4}(E), 2×10^{-3}(J) and 4×10^{-3}(N) and are much smaller than unity. Therefore the approximation of hydrostatic equilibrium is very good. Further, the change of hydrostatic pressure due to the displacement, δ_1, is smaller by a factor $\rho_g/\rho_d=\varepsilon^{-1}$ than the change of the pressure due to the gravitational force exerted on the dust in a region between h and $h+\delta_1$. This factor is sufficiently smaller than unity (see Table II(b)); therefore, the change of the gas pressure, P_{ge}, can be neglected.

References

1) V. S. Safronov, *Evolution of the Protoplanetary Cloud and Formation of the Earth and Planets* (Nauka, Moscow, 1969), English transl. NASA TT-F-677 (Springfield, Va., 1972).
2) C. Hayashi, K. Nakazawa and I. Adachi, Publ. Astron. Soc. Japan **29** (1977), 163.
H. Mizuno, Prog. Theor. Phys. **64** (1980), 544.
K. Nakazawa and Y. Nakagawa, Prog. Theor. Phys. Suppl. No. 70 (1981), 11.
Y. Nakagawa, K. Nakazawa and C. Hayashi, Icarus (1983) in press.
3) K. Nakazawa, T. Komuro and C. Hayashi, submitted to Moon Planets.
T. Komuro, K. Nakazawa and C. Hayashi, in preparation.
Y. Nakagawa and C. Hayashi, in preparation.

4) A. G. W. Cameron, Moon Planets **18** (1978), 5.
W. M. Decampli and A. G. W. Cameron, Icarus **38** (1979), 367.
5) C. Hayashi, Prog. Theor. Phys. Suppl. No. 70 (1981), 35.
6) C. Hayashi, *Proceedings of the 5-th ISAS Lunar and Planetary Symposium* (Inst. of Space and Astron Sci., Tokyo, 1972).
7) P. Goldreich and W. R. Ward, Astrophys. J. **183** (1973), 1051.
8) A. Coradini, C. Federico and G. Magni, Astron. and Astrophys. **98** (1981), 173.
9) P. Goldreich and D. Lynden-Bell, Month. Notices Roy. Astron. Soc. **130** (1965), 97.
10) I. Adachi, C. Hayashi and K. Nakazawa, Prog. Theor. Phys. **56** (1976), 1756.
11) J. H. Jeans, *Astronomy and Cosmogony,* (Cambridge Univ. Press, 1928).
12) Y. Nakagawa, M. Sekiya and C. Hayashi, in preparation.